PAPER

Large-scale investigation of the effects of nucleobase sequence on fluorescence excitation and Stokes shifts of DNA-stabilized silver clusters†

Stacy M. Copp [ID] *[a,b,c] and Anna Gonzàlez-Rosell [ID] [a]

DNA-stabilized silver clusters (Ag_N-DNAs) exhibit diverse sequence-programmed fluorescence, making these tunable nanoclusters promising sensors and bioimaging probes. Recent advances in the understanding of Ag_N-DNA structures and optical properties have largely relied on detailed characterization of single species isolated by chromatography. Because most Ag_N-DNAs are unstable under chromatography, such studies do not fully capture the diversity of these clusters. As an alternative method, we use high-throughput synthesis and spectroscopy to measure steady state Stokes shifts of hundreds of Ag_N-DNAs. Steady state Stokes shift is of interest because its magnitude is determined by energy relaxation processes which may be sensitive to specific cluster geometry, attachment to the DNA template, and structural engagement of solvent molecules. We identify 305 Ag_N-DNA samples with single-peaked emission and excitation spectra, a characteristic of pure solutions and single emitters, which thus likely contain a dominant emissive Ag_N-DNA species. Steady state Stokes shifts of these samples vary widely, are in agreement with values reported for purified clusters, and are several times larger than for typical organic dyes. We then examine how DNA sequence selects Ag_N-DNA excitation energies and Stokes shifts, comment on possible mechanisms for energy relaxation processes in Ag_N-DNAs, and discuss how differences in Ag_N-DNA structure and DNA conformation may result in the wide distribution of optical properties observed here. These results may aid computational studies seeking to understand the fluorescence process in Ag_N-DNAs and the relations of this process to Ag_N-DNA structure.

1. Introduction

Certain DNA oligomers can serve as stabilizing ligands for fluorescent silver clusters[1] (Ag_N-DNAs), whose structures and optical properties are strongly tuned by DNA sequence.[2–4] Researchers have collectively reported on Ag_N-DNAs stabilized by thousands of different DNA strands, representing a diverse palette of fluorescence properties: emission spectra peaked at 450 nm to 1000 nm,[5,6] quantum yields from 3% to 93%,[7–13] Stokes shifts up to 0.73 eV (5900 cm^{-1}),[14] and light-up or color-switching behavior induced by stimuli.[15–18] These diverse and sequence-tunable fluorescent Ag_N-DNAs are promising for applications ranging from sensing[19–22] and molecular logic schemes[23] to background-free fluorescence microscopy[24–26] and nanophotonics.[10,27,28] Recent break-throughs are rapidly advancing our understanding of the structures of certain Ag_N-DNAs,[5,7,14,29–31] largely due to detailed studies of about 20 different Ag_N-DNA species purified by high performance liquid chromatography (HPLC).[32] Purification methods are critical to ensuring interrogation of a single cluster species rather than the heterogenous mixture of fluorescent and nonfluorescent products formed by Ag_N-DNA synthesis.[33] However, because a substantial fraction of Ag_N-DNAs are unstable under chromatographic separation,[3] it remains to be determined whether the purified Ag_N-DNAs are representative of the entire palette of possible Ag_N-DNAs. An alternative examination of these clusters which does not select for stability under chromatography may shed light on this issue.

Detailed compositions of 14 purified fluorescent Ag_N-DNAs have been resolved by high resolution mass spectrometry (HR-MS), including numbers of DNA template strands and total silver content (N_{tot}), which can be separated into neutral and cationic silver content (N_0 and N_+, respectively).[7] (Unpurified Ag_N-DNAs have also been characterized by

[a]Department of Materials Science and Engineering, University of California, Irvine, Irvine, CA, 92697-2585, USA. E-mail: stacy.copp@uci.edu
[b]Department of Physics and Astronomy, University of California, Irvine, IrvineCA, 92697-4575, USA
[c]Department of Chemical and Biomolecular Engineering, University of California, Irvine, Irvine, CA, 92697-2580, USA
†Electronic supplementary information (ESI) available: Fig. S1–S7, Tables S1 and S2 and experimental details. See DOI: 10.1039/d0nr08300c

HR-MS.[8,34–36]) For purified samples, total silver content ranges from $N_{tot} = 10$ to $N_{tot} = 30$ Ag atoms.[6,7,29,32] We note that N_{tot} cannot *a priori* be assumed to represent cluster size N: recent crystallographic studies find a minority of Ag atoms are attached to the DNA template but unattached to the silver cluster.[5,14,31] For other ligand-stabilized noble metal clusters, metal atoms within the cluster core are neutral in character, while metal atoms bonded to the ligands are cationic in character.[37] For fluorescent Ag$_N$-DNAs analyzed by HR-MS, just 36% to 57% of N_{tot} are in a neutral state while the remaining silvers are cationic. Nonfluorescent silver clusters have also been found, containing $N_{tot} = 5$ to $N_{tot} = 22$, with $N_0 = 2$ to $N_0 = 10$.[7,29] In both fluorescent and non-fluorescent clusters, a fraction of the cationic silvers, N_+, are likely a part of the silver cluster and mediate attachment of the cluster core to the nucleobases, while other Ag$^+$ may be unattached to the DNA template but unattached to the silver cluster itself.

Consistent with other ligand-stabilized metal clusters,[37,38] peak excitation wavelength of fluorescent Ag$_N$-DNAs scales with the number of neutral silvers, N_0, supporting the idea that these silvers form a neutral cluster core.[28,29] Compared to monolayer-protected metal clusters, which are largely globular in shape,[39] peak excitation wavelengths and extinction coefficients of Ag$_N$-DNAs scale more strongly with N_0.[7,28] Magic number values of N_0 for Ag$_N$-DNAs[29] also differ markedly from globular clusters. These characteristics support a model for HPLC-purified Ag$_N$-DNAs whereby DNA imposes a rod-like cluster geometry onto the Ag$_N$ core.[7,8,29,30,40,41] This model was recently verified by the first X-ray crystal structures of purified Ag$_N$-DNAs.[14,31,42] A prior crystal structure of an Ag$_8$-DNA formed by *in situ* crystallization is also elongated to a lesser degree,[5] agreeing with our prediction that smaller Ag$_N$-DNAs have lower aspect ratios.[28]

While understanding of Ag$_N$-DNA structure is rapidly improving for HPLC-purifiable species, less is known about Ag$_N$-DNA photophysics. Ag$_N$-DNAs luminesce by a fluorescence-like process, with 1–4 ns emission lifetimes and quantum yields >0.1 for most purified Ag$_N$-DNAs.[7–11] (This contrasts with the ~µs emission lifetimes and lower quantum yields of many phosphorescent metal clusters.[43,44]) However, the Ag$_N$-DNA luminescence process differs from the simple Jablonski diagram of organic fluorophores.[45,46] Excitation and emission spectra of pure Ag$_N$-DNAs exhibit single dominant peaks without the vibronic shoulders characteristic of organic fluorophores.[3] The broad spectral line widths of Ag$_N$-DNAs cooled to below 2 K and the linear scaling of extinction coefficients with N_0 could be consistent with an initial collective electronic excitation leading to fluorescence.[28,47–49] Ultrafast studies of a purified Ag$_{20}$-DNA discovered a sub-100 fs relaxation from an initial excited state to a lower energy state from which fluorescence occurs.[50] Such ultrafast relaxation, which accounts for most of the Stokes shift in Ag$_N$-DNAs,[9,50] is also reported for impure Ag$_N$-DNAs.[51,52] This relaxation is too rapid for typical vibrational relaxation[53] but could instead result from dephasing of a collective electronic excitation[47] or perhaps unusually rapid vibrational relaxation.

Studies of purified Ag$_N$-DNAs also suggest that DNA scaffold conformation and local dielectric environment add diversity and complexity to excited state behavior of Ag$_N$-DNAs. Purified Ag$_N$-DNAs exhibit solvatochromic behavior that is not described by the simple Onsager-based models typically used for organic fluorophores but instead depends on the specific DNA template, and, potentially, its engagement with local solvent environment.[46] Time-resolved and polarization-resolved studies of single Ag$_N$-DNAs within a polymer film find that Ag$_N$-DNA spectral properties are sensitive to slight variations in local environment.[25,41,54] In one case, removing a terminal adenosine from the DNA template of an Ag$_{16}$-DNA increases Stokes shift while leaving cluster geometry, peak absorbance energy, and quantum yield essentially unchanged.[14] Some Ag$_N$-DNAs exhibit temperature-dependent excited state relaxation[9,14] while others do not.[13] Together, these studies paint a complex picture of the range of sequence-dependent excited state behaviors, even for the subset of Ag$_N$-DNAs which survive purification.

Because most Ag$_N$-DNAs are unstable under HPLC,[3] a large-scale investigation is needed to more fully probe the spectral palette of Ag$_N$-DNAs and determine whether the few well-studied purified Ag$_N$-DNAs are generally representative of these fluorophores. We previously reported high-throughput studies of 10^3 different Ag$_N$-DNA emission spectra, uncovering the magic numbers of Ag$_N$-DNAs[29] and learning how DNA sequence selects fluorescence emission.[55–57] These studies also illustrated the challenges of high-throughput Ag$_N$-DNA characterization: ~25% of 10-base DNA strands can stabilize multiple fluorescent Ag$_N$-DNA species with distinct emission peaks.[55] Here, we develop a method to rapidly screen steady state fluorescence excitation and emission spectra of Ag$_N$-DNAs. Motivated by studies showing that purified Ag$_N$-DNAs and single Ag$_N$-DNA emitters exhibit single excitation and emission peaks in the visible to near-infrared (NIR) spectrum,[28,30,32,47,58] we identify solutions likely to contain one dominant fluorescent Ag$_N$-DNA species by using spectral purity as an alternative to harsh purification methods. Performing Ag$_N$-DNA synthesis and steady-state fluorimetry identically on 1880 different 10-base DNA oligomers, we find 305 samples which exhibit single excitation and emission peaks. Stokes shifts of these "spectrally pure" samples vary widely, roughly increasing with peak excitation and emission energies, and generally agree with values for purified Ag$_N$-DNAs. Stokes shifts are several times larger than for typical organic fluorophores, despite comparable quantum yields of organic fluorophores and Ag$_N$-DNAs.[7–11,25] Examining the distribution of Stokes shift *versus* excitation energy, we observe two separate groupings. We hypothesize that these groupings, which appear correlated with the magic cluster sizes of Ag$_N$-DNAs,[29] arise from structural differences, apart from size only, between smaller, green-emissive Ag$_N$-DNAs and larger, red- or NIR-emissive Ag$_N$-DNAs, resulting in differences in excited state relaxation. Correlations of DNA sequence with Ag$_N$-DNA excitation energy and Stokes shift suggest that the primary role of nucleobase sequence is to select silver cluster size and exci-

tation spectrum; more subtle sequence patterns may vary the magnitude of Stokes shift for clusters of equal size by varying cluster geometry. Finally, we observe 180 Ag$_N$-DNA species with single emission peaks but two or more excitation peaks, which may arise from variations in silver cluster geometry, pointing to the diversity of the full palette of possible Ag$_N$-DNAs.

2. Methods

2.1 Silver cluster synthesis

The 1880 10-base DNA oligomers studied here were subjects of previous studies.[29,55–57] A robotic liquid handler was used to perform parallel Ag$_N$-DNA synthesis in 384 well microplates (described in ESI† and past work[29,56]). To summarize, an aqueous solution of AgNO$_3$ and NH$_4$OAc, pH 7, is mixed *via* pipetting with an aqueous solution of DNA (Integrated DNA Technologies, standard desalting). After 18 minutes, silver-DNA solutions are reduced by a freshly prepared solution of NaBH$_4$ in H$_2$O. Final stoichiometries (20 μM DNA, 10 mM NH$_4$OAc, 100 μM AgNO$_3$, and 50 μM NaBH$_4$) were selected to maximize the number of brightly fluorescent wells and the range of fluorescence colors for 10-base DNA oligomers.[55] Well plates were stored in the dark at 4 °C until measurement 7 days after synthesis. Thus, measured products in this study are time-stable to at least one week.

2.2 Spectroscopy and spectral analysis

Emission and excitation spectra were collected with a Tecan Infinite M200 PRO, whose software corrects for lamp profile and detector spectral responsivity. First, 280 nm light was used to universally excite all Ag$_N$-DNA species.[59] Emission spectra were collected from 400 nm to 800 nm (detector sensitivity is significantly limited above ~800 nm). A custom routine in Igor Pro (Wavemetrics Inc.) identified wells with single dominant fluorescent products, specifically with emission spectra well-fitted to single Gaussians as a function of energy, with peak energy E_{em} and full width at half maximum < 0.5 eV (threshold chosen by investigating previously reported linewidths of HPLC-purified Ag$_N$-DNA solutions[7]). For samples satisfying these criteria, excitation spectra were collected by monitoring emission at the fitted peak emission wavelength, $\lambda_{em} = hc/E_{em}$, while scanning excitation from 230 nm to ($\lambda_{em} - 40$ nm). The portion of each excitation spectrum above 330 nm (Region 1, Fig. 1) was fitted as a function of energy to a single Gaussian to determine peak excitation energy E_{ex}. The ultraviolet (UV) portion < 306 nm (Region 2, Fig. 1), corresponding to cluster excitation *via* the DNA,[59] was fitted to another single Gaussian. After numerically screening the numbers of peaks and sizes of standard fitting errors to flag outliers, each fit was examined by eye to determine if spectra are truly single Gaussians. For samples whose excitation and emission spectra both exhibit single Gaussian peaks in Region 1, Stokes shift is calculated as $SS = E_{ex} − E_{em}$. To compare the relative fluorescence excitation efficiencies in Regions 1 and 2 (Fig. 1), we define the ratio of these peak areas, $R_{UV/vis}$ = (area of Region 2 peak)/(area of

Fig. 1 Prototypical excitation (dashed black line) and emission (solid black line) spectra for an Ag$_N$-DNA with single excitation and emission peaks. The emission spectrum is fitted to a single Gaussian (red shading) to determine peak emission energy, E_{em}. The excitation spectrum is fitted to two single Gaussian peaks, one in the visible-NIR region at fitted peak energy, E_{ex} (green shaded fit in Region 1), and one in the UV (purple shaded fit in Region 2). Signal between 306−330 nm is excluded due to stray light in some regions of the well plate from an imperfection in the plate reader. Stokes shift, SS, is calculated as $SS = E_{ex} − E_{em}$. The ratio of excitation peak areas in Regions 1 and 2 is defined as $R_{UV/vis}$ = (area of green Region 2 peak)/(area of purple Region 1 peak). Fig. S7† shows additional excitation spectra of samples excluded from analysis due to multiple peaks in excitation or emission spectra.

Region 1 peak), where each peak area is calculated as the product of fitted peak height and fitted peak full width at half maximum. Data is listed in Table S2.†

3. Results and discussion

Ag$_N$-DNAs are well-suited for rapid fluorescence emission spectroscopy due to the universal UV excitation of these clusters *via* the nucleobases. UV excitation of solutions of a single fluorescent Ag$_N$-DNA species (excitation in Region 2, Fig. 1) produces emission spectra of the same line shapes as excitation at the cluster's specific visible-to-NIR excitation peak (green peak in Region 1, Fig. 1).[59] We exploit universal UV excitation for high-throughput spectroscopy to identify samples with single-peaked excitation and emission spectra in Region 1 (Fig. 1). We term this characteristic "spectral purity". HPLC-purified Ag$_N$-DNAs with monodisperse sizes are characterized by (i) emission spectra with single Gaussian peaks with < 0.5 eV linewidths in Region 1,[7,32] and (ii) excitation spectra with two main peaks: a Gaussian peak corresponding to direct excitation of the silver cluster[3] (Fig. 1 Region 1) and a UV peak corresponding to indirect excitation of the cluster *via* the nucleobases[59] (Region 2). Spectral purity in Region 1 can serve as an alternative to harsh chromatographic purification, identifying as-synthesized samples with spectral properties similar to purified Ag$_N$-DNA solutions or to single Ag$_N$-DNA emitters.[47,58] For these spectrally pure Ag$_N$-DNA samples, Stokes shift is $SS = E_{ex} − E_{em}$, the difference between peak excitation energy E_{ex} in Region 1 and peak emission energy E_{em}.

To identify DNA strands which host single dominant fluorescent species, we scanned UV-excited emission spectra of all 1880 Ag_N-DNA samples, finding 485 samples with emission spectra well-fitted by a single Gaussian peak of narrow linewidth as a function of energy. Remaining DNA strands either stabilized multiple emissive Ag_N-DNA species, weakly emissive Ag_N-DNAs near or below the detector's signal-to-noise ratio, or no detectable fluorescent Ag_N-DNAs (this study cannot comment on the many Ag_N-DNAs luminescent above ~800 nm,[6,60] the effective upper limit of our detector). We then collected excitation spectra in Regions 1 and 2 for the 485 DNA strands by monitoring emission signal at each sample's fitted E_{em} (see Methods). 305 of these exhibit single Gaussian excitation peaks centered at E_{ex} in Region 1. The remaining 180 samples with single peaked emission spectra but poorly resolved or multi-peaked excitation spectra are discussed in Section 3.5; because we cannot accurately assign SS in such cases, these samples are excluded from Fig. 2–6. We do not analyze linewidths here because the described method cannot distinguish single Ag_N-DNAs species with broad linewidths from multiple Ag_N-DNA species with very closely spaced energies.

3.1 Stokes shifts of spectrally pure Ag_N-DNAs

For the 305 spectrally pure samples which may be reasonably assigned to a single Ag_N-DNA species, E_{em} scales roughly linearly with E_{ex} (Fig. 2a). Such scaling is also characteristic of fluorescent organic dyes.[61] The distribution of (E_{ex}, E_{em}) values for spectrally pure samples are comparable to those reported for purified Ag_N-DNAs (cyan squares, Fig. 2a).

The multimodal histograms of E_{ex} and E_{em} (Fig. 2b and c) are expected due to the enhanced stabilities of certain Ag_N-DNAs with "magic numbers" of neutral silver atoms, N_0.[29] This magic number behavior has been shown to result in a bimodal distribution of E_{em} in the visible spectrum, which agrees with Fig. 2c. Fig. 2b shows that the distribution of E_{ex}, which has not previously been reported for 10^2 Ag_N-DNAs, is also multi-peaked. Comparison of the peaks in Fig. 2b with measured E_{ex} for magic number Ag_N-DNAs (colored lines, Fig. 2b) suggests that, just as for peak emission, magic sizes of Ag_N-DNAs lead to enhanced abundances of certain excitation energies due to the strong correlation reported between N_0 and E_{ex}.[7,28–30] Two of the purified Ag_N-DNAs with E_{ex} and E_{em} presented in Fig. 2b and c are stabilized by 10-base DNA strands within the 1880 studied in high throughput here. One of these, a red-emissive Ag_N-DNA with $N_0 = 6$, was identified as spectrally pure in our high-throughput studies. The second, a green-emissive Ag_N-DNA with $N_0 = 4$, exhibits a small secondary green emission peak (this secondary product may be removed by HPLC) and was therefore excluded from the set of spectrally pure Ag_N-DNAs.[29] HR-MS studies of additional Ag_N-DNAs may further explain the distribution in Fig. 2b, especially in the 1.9–2.4 eV range where multiple peaks may suggest distinct cluster sizes and/or geometries.

To investigate the energy relaxation process in Ag_N-DNAs, we examine the distribution of steady-state Stokes shifts, SS, of the 305 spectrally pure Ag_N-DNAs. Past high-throughput studies of Ag_N-DNAs focused solely on E_{em},[29] but it is difficult to discern excited state behavior from $E_{em} = E_{ex} − SS$ because E_{ex} and SS are determined by distinct processes. Ag_N-DNA composition and ground state geometry determine E_{ex} (or, rather,
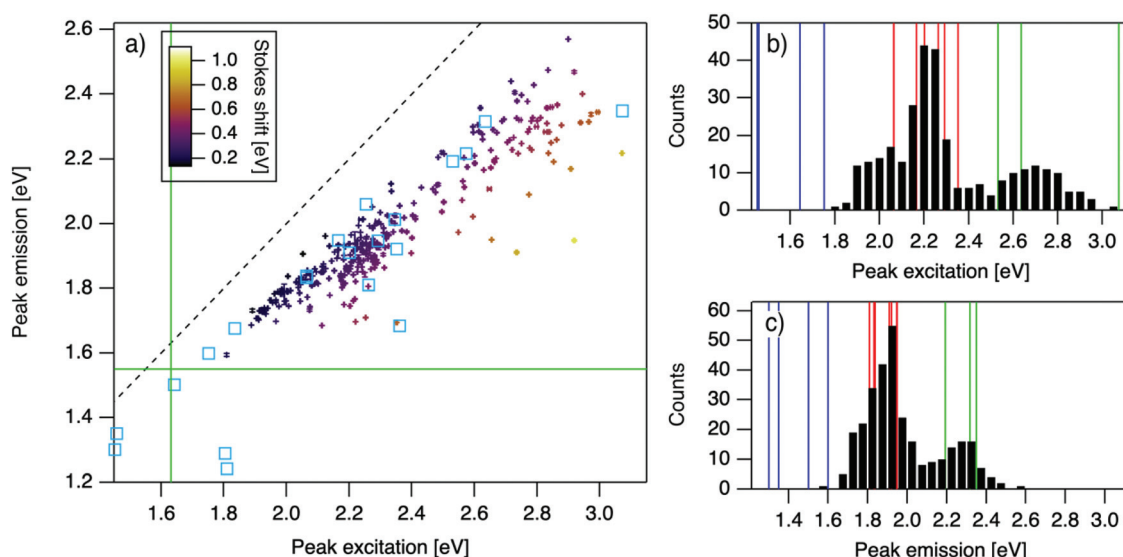

Fig. 2 (a) E_{em} versus E_{ex} for purified Ag_N-DNAs (cyan squares; data from previous studies,[6,7,11,28,29,32]) and the spectrally pure Ag_N-DNAs identified here (data points with error bars; colors correlate to Stokes shift magnitude as indicated by upper left color bar). Error bars represent standard deviations of Gaussian least squares fits. Dashed black line indicates $E_{em} = E_{ex}$, ($SS = 0$). Solid green lines are equivalent to the upper spectral wavelength limits of this study. (b and c) Histograms of (b) E_{ex} and (c) E_{em} of single-peaked Ag_N-DNA (black bars). Fourteen colored vertical lines represent (b) E_{ex} and (c) E_{em} of purified Ag_N-DNAs with $N_0 = 4$ (green), $N_0 = 6$ (red), and $N_0 = 10$ to 12 (blue), as determined by MS.[6,7,28,29]
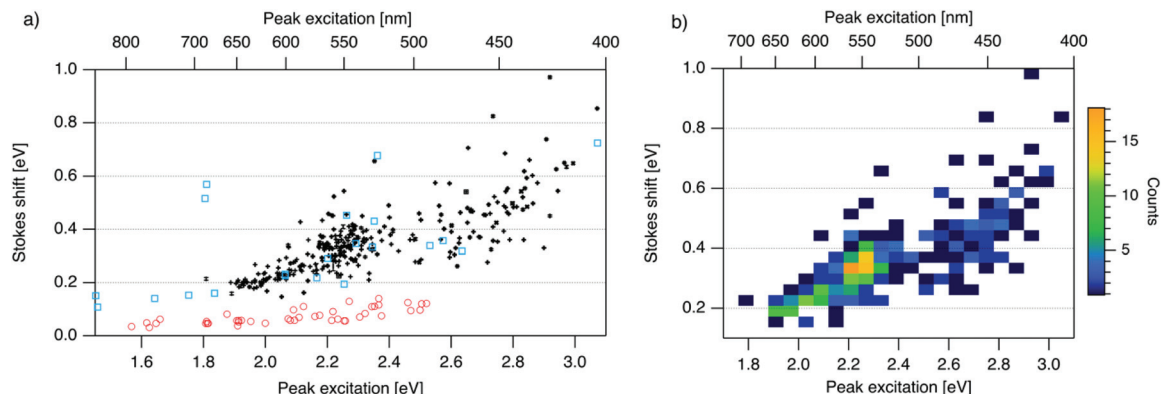
Fig. 3 (a) SS versus E_{ex} for spectrally pure solutions of Ag_N-DNAs (black), previously characterized HPLC-purified Ag_N-DNAs (cyan squares),[6,7,11,28,29,32] and organic fluorophores which are commonly used to label oligonucleotides (red circles).[81] Vertical and horizontal error bars of black points represent standard deviations; other markers are larger in size than associated standard deviations. (b) Heatmap of the data for spectrally pure Ag_N-DNAs from (a) illustrates relative abundance of certain pairs of (E_{ex}, SS) (legend indicates color meaning).

a manifold of excitation energies) required to promote the silver cluster to an initial excited state. This excited state then relaxes to a lower-energy excited state from which photoemission occurs. The energy lost between photoexcitation and photoemission determines SS. Thus, to decouple consideration of the initial excitation process from the energetic relaxation process(es), we plot SS as a function of E_{ex} (Fig. 3a). SS grows roughly linearly with E_{ex}, but SS values vary significantly for a given E_{ex}. This variance represents 10–25% of excitation energy at E_{ex} = 2.3 eV (spectral region corresponding to magic number N_0 = 6) and 10–30% at E_{ex} = 2.7 eV (corresponding to magic number N_0 = 4) (Fig. S1†). While SS variance is lesser for lower values of E_{ex}, we cannot rule out the possibility that this may be caused by reduced spectral sensitivity of the plate reader above 800 nm.

In all spectral regions, Ag_N-DNAs exhibit SS values which are several times larger than typical organic fluorophores (Table S1†), and SS also grows about four times faster with increasing E_{ex} for Ag-DNAs than for the organic fluorophores (red circles, Fig. 3a, and Fig. S2†). This behavior is remarkable considering the comparably high quantum yields of Ag_N-DNAs and organic dyes. General agreement between (E_{ex}, SS) values for HPLC-purified Ag_N-DNAs (cyan squares) and spectrally pure Ag_N-DNAs suggests that HPLC-purified Ag_N-DNAs are generally representative of excitation and emission properties of Ag_N-DNAs produced by the chemical synthesis method here.

We note that black and cyan data points at (E_{ex}, SS) ≈ (2.35 eV, 0.65 eV) represent the same DNA strand, 5′-CACCTAGCGA-3′, which stabilizes an Ag_N-DNA with exceptionally high SS, whose crystal structure was reported by Cerretani, et al.[11,31,42] Second, most of the spectrally pure Ag_N-DNAs were designed using machine learning methods.[55–57] The subset of data for DNA template strands with randomly selected DNA sequences is shown in Fig. S3.† This data generally agrees with the trend in Fig. 3a, supporting that the designed Ag_N-DNAs do not alter the (E_{ex}, SS) distribution. Fig. S4† displays a histogram of SS for spectrally pure Ag_N-DNAs with overlaid SS

values for purified Ag_N-DNAs sized by HR-MS.[6,7,28,29] N_0 and N_+ values for each of the 14 purified Ag_N-DNAs are indicated. While SS appears to increase with increasing N_+ for Ag_N-DNAs with N_0 = 6, this trend is not preserved at other N_0. With few HR-MS data available, more studies are needed to determine how N_0 and N_+ influence SS.

Because many data points overlap in Fig. 3a, a heat map in Fig. 3b quantifies abundance of (E_{ex}, SS) values, showing that data form two distinct groupings below and above E_{ex} = 2.45 eV. These two populations align with E_{ex} values of magic number sizes of HPLC-purified Ag_N-DNAs: E_{ex} > 2.5 eV corresponds to N_0 = 4 neutral Ag atoms, and 2.0 eV < E_{ex} < 2.4 eV corresponds to N_0 = 6 (Fig. 2b, vertical colored lines).[28,29] It is reasonable to hypothesize that energy relaxation following initial excitation would differ somewhat for distinct sizes of clusters due to differences in energy loss mechanisms. Crystal structures of Ag_N-DNAs, while few, suggest that a structural difference between N_0 = 4 and $N_0 \geq 6$ Ag_N-DNAs exists, beyond size only. Huard, et al., found an elongated, planar structure for an Ag_8-DNA with 450 nm maximum absorption.[5] N_0 is unknown for this Ag_8-DNA, but it is spectrally similar to N_0 = 4 Ag_N-DNAs, and a similar planar structure was suggested by a computational study for a 4-electron cluster.[62] Cerretani, et al., reported cylindrical structures for several Ag_{16}-DNAs.[14,31,42] These Ag_{16}-DNAs also lack assigned N_0 but have E_{ex} and E_{em} consistent with $N_0 \geq$ 6 Ag_N-DNAs. Combined with the trend of SS versus E_{ex} of the 305 spectrally pure Ag_N-DNAs, these few reported crystal structures could support that the silver cluster structure undergoes a planar-to-cylindrical transition between N_0 = 4 and N_0 = 6. Such a structural transition would change the number of nearest-neighbor bonds formed between Ag atoms in the cluster, possibly resulting in different energy relaxation for these two structures. Future studies are needed to test this hypothesis.

3.2 Comparison of direct and indirect Ag_N-DNA excitation

In addition to direct excitation of the silver cluster at the visible/NIR excitation peak E_{ex} which depends on cluster struc-
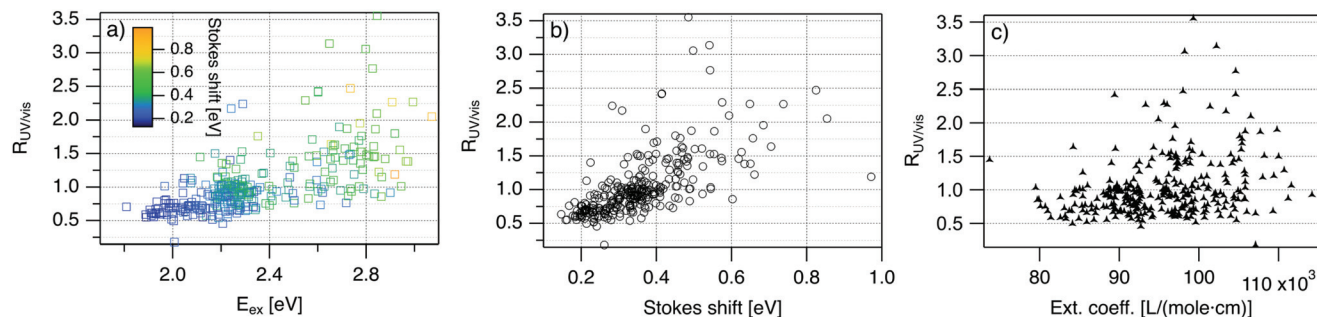
Fig. 4 $R_{UV/vis}$, ratio of areas of UV excitation peak (Region 2) to excitation peak (Region 1), as a function of (a) E_{ex}, (b) SS, and (c) extinction coefficient of the template DNA strand, calculated using the nearest neighbor model.[64,65]

ture,[3] the same Ag_N-DNA fluorescence can be excited indirectly *via* the nucleobases, which absorb most efficiently at 260–280 nm.[59] This UV excitation enables rapid emission spectroscopy of Ag_N-DNA[29] but remains poorly understood. For purified fluorescent Ag_N-DNAs, direct and indirect excitation produce emission spectra with identical shapes and linewidths.[59] One study reported ultrafast energy transfer from DNA bases to Ag_N-DNAs following UV-excitation,[63] but the authors are not aware of studies directly comparing lifetimes or quantum yields of direct *versus* indirect excitation of Ag_N-DNA fluorescence.

To investigate the UV-excited fluorescence process of Ag_N-DNAs, we compare the excitation efficiencies of indirect and direct excitation. We use the ratio of indirect to direct excitation peak areas, $R_{UV/vis}$, as a *relative* metric of excitation efficiency. The absolute excitation peak area, which is determined by a combination of extinction coefficient, fluorescence quantum yield, and chemical yield of Ag_N-DNA synthesis, cannot be used to compare multiple samples because an Ag_N-DNA species produced in high synthesis yield but with low extinction coefficient and low quantum yield is indistinguishable from an Ag_N-DNA species produced in low synthesis yield with high extinction coefficient and high quantum yield. Instead, a relative comparison of excitation peaks in Regions 1 and 2 (Fig. 1) using the metric $R_{UV/vis}$ allows us to decouple chemical yield from other factors determining excitation efficiency.

Fig. 4 displays $R_{UV/vis}$ as a function of E_{ex}, SS, and extinction coefficient. On average, $R_{UV/vis}$ increases with increasing E_{ex}, corresponding to greater UV excitation efficiency of smaller clusters with larger E_{ex} than of larger clusters with lower E_{ex} (Fig. 4a). $R_{UV/vis}$ also generally increases as SS increases (Fig. 4b); this is expected due to the trend of SS *versus* E_{ex} in Fig. 3, but $R_{UV/vis}$ does trend more strongly with SS than with E_{ex}. $R_{UV/vis}$ does not depend strongly on extinction coefficient of the DNA template strand, which is a function of nucleobase content (Fig. 4c, calculated using the nearest neighbor model.[64,65]). Thus, trends in Fig. 4 are not only due to how well the DNA template absorbs UV photons but also to the properties of silver clusters themselves.

The correlation of $R_{UV/vis}$ with E_{ex} can be rationalized by two factors. First, Ag_N-DNA cluster core size, N_0, increases as E_{ex} decreases.[29] Because visible-NIR extinction coefficients of Ag_N-DNAs scale linearly with N_0,[28] visible-NIR excitation peak area will increase as E_{ex} decreases, causing $R_{UV/vis}$ to decrease as E_{ex} decreases. Second, UV excitation may be more efficient for smaller, greener Ag_N-DNAs than for larger, redder clusters due to increased overlap of small clusters' energy levels with the nucleobase energy levels. More detailed studies, such as time-resolved infrared spectroscopy to monitor nucleobase excitations,[66] could investigate whether one or both of these factors determine the behavior in Fig. 4a.

The correlation of $R_{UV/vis}$ with SS is, in large part, due to the linear correlation of SS with E_{ex} (Fig. 3a). We speculate that the slightly stronger correlation of $R_{UV/vis}$ with SS than with E_{ex} may be caused by stronger coupling of smaller, greener clusters with the DNA, resulting in greater energy relaxation relative to larger clusters. Significant spread of $R_{UV/vis}$ values for a single SS or E_{ex} value may arise from variations in cluster attachment to the DNA, *e.g.*, the strength of coupling of the cluster to the nucleobases. Further studies are needed to determine the origin of this spread.

3.3 Role of base sequence in selecting Ag_N-DNA optical properties

Improved understanding of the sequence-dependence of Ag_N-DNAs can enable rational design of fluorophores with custom properties. We previously applied data mining and machine learning to a data library of 10^3 DNA sequences to uncover nucleobase patterns ("motifs") correlated with the value of E_{em}.[56] When combined with machine learning, these motifs are effective building blocks for designing new Ag_N-DNAs with desired values of E_{em}.[56,57] To also investigate how DNA sequence selects E_{ex}, SS, and $R_{UV/vis}$, we analyze correlations of DNA base motifs to values of E_{ex}, E_{em}, SS, and $R_{UV/vis}$. (305 spectrally pure Ag_N-DNAs is rather few for machine learning, so we examine statistical correlations of base patterns with Ag_N-DNA optical properties.)

Fig. 5 displays mean values of E_{ex}, E_{em}, SS, and $R_{UV/vis}$ for single nucleobases (A, C, G, T) and two-base motifs in the 305 spectrally pure Ag_N-DNA template sequences (means are

Fig. 5 Mean values of (a) E_{ex}, (b) E_{em}, (c) SS, and (d) $R_{UV/vis}$ for each instance of the four nucleobases and the 16 possible two-base motifs in the set of DNA template sequences for the 305 spectrally pure Ag$_N$-DNAs. Error bars represent standard error, as a measure of precision of the mean.

weighted by number of occurrences of each base pattern in a given DNA sequence). Fig. S5† also displays means for three-base motifs. Correlations of DNA sequence with E_{em} (Fig. 5b) agree with previous findings[56,57] that A-rich motifs are correlated with greener emission (higher energies) and consecutive G's are strongly correlated with redder emission (lower energies). This agreement is expected because the 305 spectrally pure Ag$_N$-DNAs were included in those previous studies. The association of smaller, greener clusters with A-rich motifs and larger, redder clusters with G-rich motifs has been suggested

to arise from varying affinities of silver cations for different nucleobases.[67]

We observe that relative trends of mean E_{ex}, E_{em}, SS, and $R_{UV/vis}$ values in Fig. 5 are similar to one another. (Because E_{em} is a linear combination of E_{ex} and SS, this similarity is expected for E_{em}.) In Fig. 5a, c, and d, nucleobases A and T are associated with higher values of E_{ex}, SS, and $R_{UV/vis}$, while G is associated with lower values of each of these parameters. Trends for two-base motifs are also similar among all parameters, with some distinct differences for $R_{UV/vis}$. This trend is expected given roughly linear correlations of SS and $R_{UV/vis}$ with E_{ex} (Fig. 2a, 3a and 4a) and shows that DNA sequence patterns which select for the excitation energy E_{ex} from ground state to initial unrelaxed excited state (Franck Condon state) are also predictive of the magnitude of SS, the energy lost during relaxation following excitation. A lack of obviously distinct sequence patterns which encode SS and E_{ex} could support that energy relaxation is due to a delocalized relaxation across the entire cluster and/or DNA template, as opposed to specific relaxation of one or a few excited nucleobases. Because E_{ex}, SS, and $R_{UV/vis}$ do not appear to be separately tuned by distinct DNA base motifs to a significant degree, designing an Ag$_N$-DNA with custom values for each of these optical properties is likely to be a significant challenge, although three-base motifs may enable such prediction (Fig. S5†), which is the subject of ongoing work.

To elucidate if subtler sequence features determine SS irrespective of E_{ex}, we consider the most abundant peak in Fig. 2b: 2.15 eV < E_{ex} < 2.45 eV. HPLC-purified Ag$_N$-DNAs in this spectral range have N_0 = 6 neutral Ag atoms. The 145 DNA sequences in this peak are separated into two categories above and below their median SS value (Fig. 6a). Average numbers of nucleobase, 2-base, and 3-base patterns are calculated for both categories. Fig. 6b and c display average numbers of bases and 2-base motifs in sequences correlated to higher (orange) and lower (green) SS categories, with base patterns ordered left-to-right in order of the relative difference between average occurrence in the two classes, which is a metric of predictiveness of SS value for each base pattern (3-base patterns in Fig. S6†). For this specific spectral window, inclusion of T bases generally increases SS, while A and G bases tend to reduce SS. Interestingly, A-rich motifs were correlated to higher SS values when considering the entire 305 spectrally pure Ag$_N$-DNAs, but
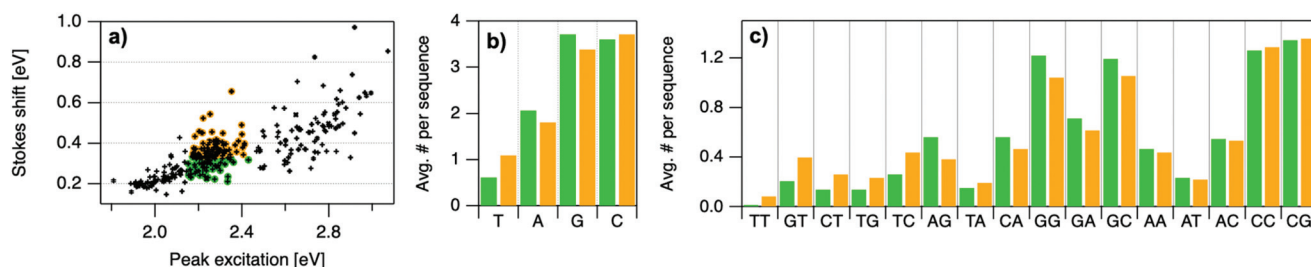

Fig. 6 (a) Indication of low SS (green) and high SS (orange) categories, separated at the median value of SS = 0.336 eV. b, (c) Motifs are sorted left to right in order of greatest relative difference between orange and green bars.

their role for selecting *SS* for a given color window may be more nuanced. C is less predictive of *SS*, and behavior of 2-base motifs containing C's is generally predicted by A, G, and T content.

The differences in *SS* behavior of Ag$_N$-DNAs stabilized by A- and G-rich strands as compared to T-rich strands are somewhat unexpected if one assumes that strength of silver-nucleobase bonds should control *SS* magnitude. Thymines are not expected to bind the silver cluster and adenines are expected to bind rather weakly, as compared to strong affinities of cytosine and guanine for silver.[67,68] The few crystal structures available for Ag$_N$-DNAs show that A can coordinate the silver cluster,[69] although a separate study of a DNA-Ag$^+$ complex finds that adenines protrude outward from Ag$^+$-mediated DNA duplexes.[5,14,31] T is similarly observed to protrude away from silver clusters.[70] While solved Ag$_N$-DNA structures are scant and may not be representative of general behavior, we note that differences in *SS* of Ag$_N$-DNAs in Fig. 6 do not appear to be explained simply by total silver-binding power of the DNA template, due to the similar *SS* values correlated with A- and G-rich motifs. The relaxation dynamics of a more tightly bound cluster would be expected to differ from a weakly bound cluster. Since G likely binds to the cluster more strongly than A, this simple model is unlikely.

Other possible mechanisms for finer variations in *SS* behavior include cluster structural variations and slight differences in vibrational modes of nucleic acids, which are measured in the range of 0.19 eV to 0.21 eV.[14,31] Thymine has the highest frequency modes of the set of natural nucleobases in DNA,[71] which could increase *SS* of T-containing Ag$_N$-DNAs if energy relaxation occurs *via* vibrational modes (discussed below). A and G are both purines with bulkier sizes than T, which may affect energy relaxation of the excited cluster. It is unclear whether the vibrational modes of free nucleobases are representative of silver-bound nucleobases, and more crystal structures must be solved to understand how structure contributes to *SS* and how the four nucleobases coordinate silver clusters.

3.4 Possible origins of the Stokes shift in Ag$_N$-DNAs

By the Franck-Condon principle, *SS* is determined by processes which follow photoexcitation.[71] Possible mechanisms for energy relaxation processes in Ag$_N$-DNAs include electronic dephasing, vibrational relaxation, and charge transfer. Measured vibrational modes of nucleic acids, 0.19 eV to 0.21 eV,[72] roughly correspond to the lower limit of *SS* values observed (Fig. 3a), which could support an energetic relaxation process *via* excitation of one or more vibrational modes in the nucleic acids of the surrounding DNA ligand. However, vibrational modes of nucleic acids bound to silver cations may differ from free nucleic acids. Calculations by Weerawardene and Aikens for thiolate-protected gold clusters found that changes in cluster geometry after excitation, *i.e.* nuclear rearrangement of Au atoms, lead to electronic structure changes that produce a Stokes shifts, and the magnitude of these geometric changes are correlated to the magnitude of *SS*.[53] Calculations of thiolate-protected Ag clusters also find

geometric relaxation following excitation with a magnitude that is smaller for larger clusters, leading to inverse correlation of cluster size and *SS*[73–75] which matches what is observed here for Ag$_N$-DNAs.

The extremely rapid 10–100 fs energy relaxation observed immediately following Ag$_N$-DNA excitation[45] may be too fast to be caused solely by geometric relaxation of cluster and/or DNA ligand structure or by charge transfer.[50–52] However, *ab initio* calculations of small atomic chains of Ag atoms found ~100 fs plasmon dephasing due to certain molecular vibrations in 1-dimensional atomic Ag chains.[71] Thus, the unusual ultrafast energy relaxation process in Ag$_N$-DNAs may be of mixed character, involving both electronic dephasing and geometric relaxation. A recent study used ultrafast time-resolved infrared spectroscopy to monitor vibrational modes of DNA nucleobases following excitation of two green-emissive Ag$_N$-DNAs at their visible excitation wavelengths. Upon excitation, vibrational modes of certain nucleobases were found to bleach.[76] Because isolated nucleobases require higher energy (UV) excitation to undergo bleaching, this suggests an intimate and intriguing connection between the silver cluster and its nucleobase ligands. Future studies are needed to understand how electronic dephasing, vibrational relaxation, and/or charge transfer contribute to the origins of Stokes shift in Ag$_N$-DNAs. Such studies could shed light on why Ag$_N$-DNAs retain high quantum yields and *SS* values several times larger than organic fluorophores, even into the NIR.[66]

3.5 Multipeaked excitation spectra: heterogeneous samples or fundamentally different Ag$_N$-DNA structures?

Of the 485 Ag$_N$-DNA samples which exhibited single-peaked emission spectra, 305 of these also exhibited single-peaked excitation spectra (*e.g.* Fig. 1) while the remaining 180 samples exhibited excitation spectra with poorly resolved peaks, asymmetric peaks or, for 88 samples, multiple peaks > 350 nm. Fig. S7† illustrates representative examples of these excitation spectra. The most common secondary peak observed was in the near UV between the nucleobase absorption band and the dominant Region 1 peak (Fig. 1); this peak appeared in 63 samples. While it is most convenient to simply dismiss these samples as heterogeneous mixtures of different clusters indiscernible by emission spectra only (which is reasonable for poorly resolved or asymmetric peaks), we cannot rule out the possibility that some multipeaked samples may represent single Ag$_N$-DNA species with spectral features which fundamentally differ from the well-studied HPLC-stable Ag$_N$-DNAs with single Gaussian excitation peaks in Region 1 (Fig. 1). As described in Methods, all measurements were performed one week after Ag$_N$-DNA synthesis to capture only time-stable products. Ag$_N$-DNAs evolve in the hours to few days after synthesis but generally stabilize well before one week.[13] Thus, it is unlikely that Ag$_N$-DNAs undergo significant evolution in size/shape during collection of emission spectra and excitation spectra, which would could cause the appearance of multiple excitation peaks. Another possible cause of Ag$_N$-DNAs with single-peaked emission spectra but multipeaked excitation

spectra is when a single DNA template strand forms two different Ag_N-DNA species with equal E_{em}, one with low SS and one with high SS. The probability of this occurring in such a large fraction of samples is highly unlikely. Finally, larger silver nanoparticles display size-dependent surface plasmon resonances,[77] but excitation of surface plasmons in nanoparticle impurities should not induce fluorescence in separate Ag_N-DNAs that coexist in solution.

A final possibility is that certain Ag_N-DNAs inherently have multipeaked excitation spectra, with a dominant visible-NIR peak and a secondary peak, typically between 3 eV and 3.5 eV. Secondary excitation peaks at 3–3.5 eV have been observed in a few HPLC-purified Ag_N-DNAs.[78] A particularly stable and bright Ag_N-DNA which emits at 670 nm has a primary excitation peak at 600 nm and a secondary excitation peak at 400 nm.[28] Secondary excitation peaks at energies $>E_{ex}$ are consistent with fluorescence arising from an initial collective excitation in Ag_N-DNAs.[10] In this model, the dominant visible-NIR excitation peak corresponds to a longitudinal collective electronic oscillation along the silver cluster rod. In this rod, a transverse collective mode is also expected. Computational studies find that this mode is damped in straight atomic Ag chains,[28] but simulations of atomic Ag chains with chiral twist find that as chirality increases, transverse excitation peaks become more prominent.[79] We hypothesize that some Ag_N-DNAs with increased curvatures host more prominent transverse excitation modes which also lead to Ag_N-DNA fluorescence. Ag_N-DNAs with higher curvature may not have been observed in large numbers due to lower stabilities under HPLC as compared to straighter Ag_N-DNAs.

4. Conclusions

We present the first high-throughput study probing Stokes shifts of Ag_N-DNAs across the diverse spectral range of these nanoclusters. By using spectral purity to identify 305 samples containing a single fluorescent Ag_N-DNA species, we found that Stokes shifts for these samples vary widely and are several times larger than organic fluorophores, despite the molecular-like high quantum yields of Ag_N-DNAs.[30,80] The distribution of peak excitation energies and Stokes shifts suggests that there may exist distinctions between excited state relaxation processes in Ag_N-DNAs with $N_0 = 4$ and $N_0 \geq 6$ neutral Ag atoms. By comparing to crystal structures available for Ag_N-DNAs,[5,14,31,42] we propose that Ag_N-DNA cluster structure transitions from planar to cylindrical between $N_0 = 4$ and $N_0 = 6$, resulting in different magnitudes of energy relaxation following photoexcitation. Future studies are needed to test this hypothesis.

We also found strong correlations between certain DNA sequence patterns and peak excitation energy. Because Stokes shift scales strongly with excitation energy, sequence patterns predictive only of Stokes shift but not of excitation energy are more subtle. This suggests that the primary role of DNA sequence is to select the silver cluster's structure, which plays the dominant role in determining the energy relaxation process following photoexcitation. Finer variations of cluster geometry and/or the cluster's interaction with its DNA template may cause the significant spread of Stokes shifts observed for Ag_N-DNAs with equal excitation energies. Finally, we observe a significant minority of Ag_N-DNAs with single-peaked emission spectra yet multiple peaks in excitation spectra, particularly in the near UV. The prevalence of these samples, and the near UV energies of their peaks, could correspond to transverse collective excitation modes of clusters with greater chirality, as predicted by *ab initio* calculations.[5,14,31] We hope that the extensive data set presented here will enable computational studies of fluorescence excitation and emission processes in Ag_N-DNAs.

Conflicts of interest

There are no conflicts to declare.

Notes and references

1 J. T. Petty, J. Zheng, N.,V. Hud and R. M. Dickson, DNA-templated Ag nanocluster formation, *J. Am. Chem. Soc.*, 2004, **126**, 5207–5212.

2 E. G. Gwinn, P. O'Neill, A. J. Guerrero, D. Bouwmeester and D. K. Fygenson, Sequence-Dependent Fluorescence of DNA-Hosted Silver Nanoclusters, *Adv. Mater.*, 2008, **20**, 279–283.

3 E. G. Gwinn, D. Schultz, S. M. Copp and S. M. Swasey, DNA-Protected Silver Clusters for Nanophotonics, *Nanomaterials*, 2015, **5**, 180–207.

4 Y. Chen, M. L. Phipps, J. H. Werner, S. Chakraborty and J. S. Martinez, DNA Templated Metal Nanoclusters: From Emergent Properties to Unique Applications, *Acc. Chem. Res.*, 2018, **51**, 2756–2763.

5 D. J. E. Huard, *et al.*, Atomic Structure of a Fluorescent Ag8 Cluster Templated by a Multistranded DNA Scaffold, *J. Am. Chem. Soc.*, 2019, **141**, 11465–11470.

6 S. M. Swasey, et al., High throughput near infrared screening discovers DNA-templated silver clusters with peak fluorescence beyond 950 nm, Nanoscale, 2018, 10, 19701–19705.

7 D. Schultz, et al., Evidence for rod-shaped DNA-stabilized silver nanocluster emitters, Adv. Mater., 2013, 25, 2797–2803.

8 J. T. Petty, M. Ganguly, I. J. Rankine, D. M. Chevrier and P. Zhang, A DNA-Encapsulated and Fluorescent Ag_{10}^{6+} Cluster with a Distinct Metal-Like Core, J. Phys. Chem. C, 2017, 121, 14936–14945.

9 C. Cerretani, M. R. Carro-Temboury, S. Krause, S. A. Bogh and T. Vosch, Temperature dependent excited state relaxation of a red emitting DNA-templated silver nanocluster, Chem. Commun., 2017, 53, 12556–12559.

10 S. A. Bogh, C. Cerretani, L. Kacenauskaite, M. R. Carro-Temboury and T. Vosch, Excited-State Relaxation and Förster Resonance Energy Transfer in an Organic Fluorophore/Silver Nanocluster Dyad, ACS Omega, 2017, 2, 4657–4664.

11 S. A. Bogh, et al., Unusually large Stokes shift for a near-infrared emitting DNA-stabilized silver nanocluster, Methods Appl. Fluoresc., 2018, 6, 024004.

12 P. R. O'Neill, L. R. Velazquez, D. G. Dunn, E. G. Gwinn and D. K. Fygenson, Hairpins with Poly-C Loops Stabilize Four Types of Fluorescent Ag n, DNA, 2009, 4229–4233.

13 V. A. Neacșu, et al., Unusually large fluorescence quantum yield for a near-infrared emitting DNA-stabilized silver nanocluster, Chem. Commun., 2020, 56(47), 6384–6387.

14 C. Cerretani, J. Kondo and T. Vosch, Removal of the A10 adenosine in a DNA-stabilized Ag16 nanocluster, RSC Adv., 2020, 10, 23854–23860.

15 H.-C. Yeh, et al., A fluorescence light-up Ag nanocluster probe that discriminates single-nucleotide variants by emission color, J. Am. Chem. Soc., 2012, 134, 11550–11558.

16 M. Ganguly, C. Bradsher, P. Goodwin and J. T. Petty, DNA-Directed Fluorescence Switching of Silver Clusters, J. Phys. Chem. C, 2015, 119, 27829–27837.

17 C. Cerretani and T. Vosch, Switchable Dual-Emissive DNA-Stabilized Silver Nanoclusters, ACS Omega, 2019, 4, 7895–7902.

18 L. E. Yourston and A. V. Krasnoslobodtsev, Micro RNA Sensing with Green Emitting Silver Nanoclusters, Molecules, 2020, 25, 3026.

19 S. W. Yang and T. Vosch, Rapid detection of microRNA by a silver nanocluster DNA probe, Anal. Chem., 2011, 83, 6935–6939.

20 J. Liu, DNA-stabilized, fluorescent, metal nanoclusters for biosensor development, TrAC, Trends Anal. Chem., 2014, 58, 99–111.

21 Y.-A. Chen, et al., NanoCluster Beacons Enable Detection of a Single N(6)-Methyladenine, J. Am. Chem. Soc., 2015, 137, 10476–10479.

22 J. T. Del Bonis-O'Donnell, D. Vong, S. Pennathur and D. K. Fygenson, A universal design for a DNA probe providing ratiometric fluorescence detection by generation of silver nanoclusters, Nanoscale, 2016, 8, 14489–14496.

23 Z. Huang, Y. Tao, F. Pu, J. Ren and X. Qu, Versatile logic devices based on programmable DNA-regulated silver-nanocluster signal transducers, Chemistry, 2012, 18, 6663–6669.

24 B. C. Fleischer, J. T. Petty, J.-C. Hsiang and R. M. Dickson, Optically Activated Delayed Fluorescence, J. Phys. Chem. Lett., 2017, 8, 3536–3543.

25 S. Krause, M. R. Carro-Temboury, C. Cerretani and T. Vosch, Probing heterogeneity of NIR induced secondary fluorescence from DNA-stabilized silver nanoclusters at the single molecule level, Phys. Chem. Chem. Phys., 2018, 20, 16316–16319.

26 S. Krause, C. Cerretani and T. Vosch, Disentangling optically activated delayed fluorescence and upconversion fluorescence in DNA stabilized silver nanoclusters, Chem. Sci., 2019, 10, 5326–5331.

27 D. Schultz, et al., Dual-color nanoscale assemblies of structurally stable, few-atom silver clusters, as reported by fluorescence resonance energy transfer, ACS Nano, 2013, 7, 9798–9807.

28 S. M. Copp, D. Schultz, S. M. Swasey, A. Faris and E. G. Gwinn, Cluster Plasmonics: Dielectric and Shape Effects on DNA-Stabilized Silver Clusters, Nano Lett., 2016, 16, 3594–3599.

29 S. M. Copp, et al., Magic Numbers in DNA-Stabilized Fluorescent Silver Clusters Lead to Magic Colors, J. Phys. Chem. Lett., 2014, 5, 959–963.

30 S. M. Swasey, et al., Chiral Electronic Transitions in Fluorescent Silver Clusters Stabilized by DNA, ACS Nano, 2014, 8, 6883–6892.

31 C. Cerretani, H. Kanazawa, T. Vosch and J. Kondo, Crystal structure of a NIR-Emitting DNA-Stabilized Ag16 Nanocluster, Angew. Chem., Int. Ed., 2019, 58, 17153–17157.

32 D. Schultz and E. G. Gwinn, Silver atom and strand numbers in fluorescent and dark Ag:DNAs, Chem. Commun., 2012, 48, 5748–5750.

33 M. R. Carro-Temboury, V. Paolucci, E. N. Hooley, L. Latterini and T. Vosch, Probing DNA-stabilized fluorescent silver nanocluster spectral heterogeneity by time-correlated single photon counting, Analyst, 2016, 141, 123–130.

34 K. Koszinowski and K. A. Ballweg, Highly Charged Ag_6^{4+} Core in a DNA-Encapsulated Silver Nanocluster, Chem. – Eur. J., 2010, 16, 3285–3290.

35 J. T. Petty, M. Ganguly, I. J. Rankine, D. M. Chevrier and P. Zhang, A DNA-Encapsulated and Fluorescent Ag106+Cluster with a Distinct Metal-Like Core, J. Phys. Chem. C, 2017, 121, 14936–14945.

36 J. T. Petty, et al., Repeated and Folded DNA Sequences and Their Modular Ag106+Cluster, J. Phys. Chem. C, 2018, 122, 4670–4680.

37 H. Häkkinen, Atomic and electronic structure of gold clusters: understanding flakes, cages and superatoms from simple concepts, Chem. Soc. Rev., 2008, 37, 1847–1859.

38 M. Walter, *et al.*, A unified view of ligand-protected gold clusters as superatom complexes, *Proc. Natl. Acad. Sci. U. S. A.*, 2008, **105**, 9157–9162.

39 I. Chakraborty and T. Pradeep, Atomically Precise Clusters of Noble Metals: Emerging Link between Atoms and Nanoparticles, *Chem. Rev.*, 2017, **117**, 8208–8271.

40 N. Markešević, S. S. R. Oemrawsingh, D. Schultz, E. G. Gwinn and D. Bouwmeester, Polarization Resolved Measurements of Individual DNA-Stabilized Silver Clusters, *Adv. Opt. Mater.*, 2014, **2**, 765–770.

41 E. N. Hooley, M. R. Carro-Temboury and T. Vosch, Probing the Absorption and Emission Transition Dipole Moment of DNA Stabilized Silver Nanoclusters, *J. Phys. Chem. A*, 2017, **121**, 963–968.

42 C. Cerretani, J. Kondo and T. Vosch, Mutation of position 5 as a crystal engineering tool for a NIR-Emitting DNA-Stabilized Ag16 Nanocluster, *CrystEngComm*, 2020, **46**, 8136–8141.

43 S. Chakraborty, *et al.*, A Hybrid DNA-Templated Gold Nanocluster for Enhanced Enzymatic Reduction of Oxygen, *J. Am. Chem. Soc.*, 2015, **137**, 11678–11687.

44 R. Jin, C. Zeng, M. Zhou and Y. Chen, Atomically Precise Colloidal Metal Nanoclusters and Nanoparticles: Fundamentals and Opportunities, *Chem. Rev.*, 2016, **116**, 10346–10413.

45 J. R. Lakowicz, Principles of fluorescence spectroscopy, in *Principles of Fluorescence Spectroscopy*, Springer Science & Business Media, 2006. DOI: 10.1007/978-0-387-46312-4.

46 S. M. Copp, A. Faris, S. M. Swasey and E. G. Gwinn, Heterogeneous Solvatochromism of Fluorescent DNA-Stabilized Silver Clusters Precludes Use of Simple Onsager-Based Stokes Shift Models, *J. Phys. Chem. Lett.*, 2016, **7**, 698–703.

47 S. S. R. Oemrawsingh, N. Markešević, E. G. Gwinn, E. R. Eliel and D. Bouwmeester, Spectral Properties of Individual DNA-Hosted Silver Nanoclusters at Low Temperatures, *J. Phys. Chem. C*, 2012, **116**, 25568–25575.

48 S. Bernadotte, F. Evers and C. R. Jacob, Plasmons in Molecules, *J. Phys. Chem. C*, 2013, **117**, 1863–1878.

49 C. M. Krauter, S. Bernadotte, C. R. Jacob, M. Pernpointner and A. Dreuw, Identification of Plasmons in Molecules with Scaled Ab Initio Approaches, *J. Phys. Chem. C*, 2015, **119**, 24564–24573.

50 E. Thyrhaug, *et al.*, Ultrafast coherence transfer in DNA-templated silver nanoclusters, *Nat. Commun.*, 2017, **8**, 15577.

51 S. H. Yau, *et al.*, Bright two-photon emission and ultra-fast relaxation dynamics in a DNA-templated nanocluster investigated by ultra-fast spectroscopy, *Nanoscale*, 2012, **4**, 4247–4254.

52 S. A. Patel, *et al.*, Electron transfer-induced blinking in Ag nanodot fluorescence, *J. Phys. Chem. C. Nanomater. Interfaces*, 2009, **113**, 20264–20270.

53 D. Brinks, *et al.*, Ultrafast dynamics of single molecules, *Chem. Soc. Rev.*, 2014, **43**, 2476–2491.

54 E. N. Hooley, V. Paolucci, Z. Liao, M. R. Carro Temboury and T. Vosch, Single-Molecule Characterization of Near-Infrared-Emitting Silver Nanoclusters, *Adv. Opt. Mater.*, 2015, **3**, 1109–1115.

55 S. M. Copp, P. Bogdanov, M. Debord, A. Singh and E. Gwinn, Base Motif Recognition and Design of DNA Templates for Fluorescent Silver Clusters by Machine Learning, *Adv. Mater.*, 2014, **26**, 5839–5845.

56 S. M. Copp, *et al.*, Fluorescence Color by Data-Driven Design of Genomic Silver Clusters, *ACS Nano*, 2018, **12**, 8240–8247.

57 S. M. Copp, S. M. Swasey, A. Gorovits, P. Bogdanov and E. G. Gwinn, General Approach for Machine Learning-Aided Design of DNA-Stabilized Silver Clusters, *Chem. Mater.*, 2020, **32**, 430–437.

58 T. Vosch, *et al.*, Strongly emissive individual DNA-encapsulated Ag nanoclusters as single-molecule fluorophores, *Proc. Natl. Acad. Sci. U. S. A.*, 2007, **104**, 12616–12621.

59 P. R. O'Neill, E. G. Gwinn and D. K. Fygenson, UV Excitation of DNA Stabilized Ag Cluster Fluorescence via the DNA Bases, *J. Phys. Chem. C*, 2011, **115**, 24061–24066.

60 S. M. Swasey, *et al.*, Adaptation of a visible wavelength fluorescence microplate reader for discovery of near-infrared fluorescent probes, *Rev. Sci. Instrum.*, 2018, **89**, 095111.

61 B. Valeur and M. N. Berberan-Santos, *Molecular Fluorescence: Principles and Applications*, Wiley-VCH Verlag & Co., KGaA, 2012.

62 X. Chen, M. Boero and O. Lopez-Acevedo, Atomic structure and origin of chirality of DNA-stabilized silver clusters, *Phys. Rev. Mater.*, 2020, **4**, 065601.

63 I. L. Volkov, Z. V. Reveguk, P. Y. Serdobintsev, R. R. Ramazanov and A. I. Kononov, DNA as UV light-harvesting antenna, *Nucleic Acids Res.*, 2018, **46**, 3543–3551.

64 M. M. Warshaw and I. Tinoco, Optical properties of sixteen dinucleoside phosphates, *J. Mol. Biol.*, 1966, **20**, 29–38.

65 M. J. Cavaluzzi and P. N. Borer, Revised UV extinction coefficients for nucleoside-5′-monophosphates and unpaired DNA and RNA, *Nucleic Acids Res.*, 2004, **32**, e13.

66 Y. Zhang, C. He, J. T. Petty and B. Kohler, Time-Resolved Vibrational Fingerprints for Two Silver Cluster-DNA Fluorophores, *J. Phys. Chem. Lett.*, 2020, 8958–8963, DOI: 10.1021/acs.jpclett.0c02486.

67 S. M. Swasey, L. E. Leal, O. Lopez-Acevedo, J. Pavlovich and E. G. Gwinn, Silver(ı) as DNA glue: Ag(+)-mediated guanine pairing revealed by removing Watson-Crick constraints, *Sci. Rep.*, 2015, **5**, 10163.

68 S. M. Swasey and E. G. Gwinn, Silver-mediated base pairings: Towards dynamic DNA nanostructures with enhanced chemical and thermal stability, *New J. Phys.*, 2016, **18**, 045008.

69 S. M. Swasey, F. Rosu, S. M. Copp, V. Gabelica and E. G. Gwinn, Parallel Guanine Duplex and Cytosine Duplex

DNA with Uninterrupted Spines of AgI-Mediated Base Pairs, *J. Phys. Chem. Lett.*, 2018, **9**, 6605–6610.

70 J. Kondo, *et al.*, A metallo-DNA nanowire with uninterrupted one-dimensional silver array, *Nat. Chem.*, 2017, **9**, 956–960.

71 C. S. Peng, K. C. Jones and A. Tokmakoff, Anharmonic vibrational modes of nucleic acid bases revealed by 2D IR spectroscopy, *J. Am. Chem. Soc.*, 2011, **133**, 15650–15660.

72 L. Gell, *et al.*, Tuning Structural and Optical Properties of Thiolate-Protected Silver Clusters by Formation of a Silver Core with Confined Electrons, *J. Phys. Chem. C*, 2013, **117**, 14824–14831.

73 K. L. D. M. Weerawardene and C. M. Aikens, Theoretical Insights into the Origin of Photoluminescence of Au25(SR) 18- Nanoparticles, *J. Am. Chem. Soc.*, 2016, **138**, 11202–11210.

74 K. L. D. M. Weerawardene, E. B. Guidez and C. M. Aikens, Photoluminescence Origin of Au 38 (SR) 24 and Au 22 (SR) 18 Nanoparticles: A Theoretical Perspective, *J. Phys. Chem. C*, 2017, **121**, 15416–15423.

75 K. L. D. M. Weerawardene and C. M. Aikens, Origin of Photoluminescence of Ag 25 (SR) 18 – Nanoparticles: Ligand and Doping Effect, *J. Phys. Chem. C*, 2018, **122**, 2440–2447.

76 G. Donati, D. B. Lingerfelt, C. M. Aikens and X. Li, Molecular Vibration Induced Plasmon Decay, *J. Phys. Chem. C*, 2017, **121**, 15368–15374.

77 J. J. Mock, M. Barbic, D. R. Smith, D. A. Schultz and S. Schultz, Shape effects in plasmon resonance of individual colloidal silver nanoparticles, *J. Chem. Phys.*, 2002, **116**, 6755–6759.

78 V. Amendola, O. M. Bakr and F. Stellacci, A study of the surface plasmon resonance of silver nanoparticles by the discrete dipole approximation method: Effect of shape, size, structure, and assembly, *Plasmonics*, 2010, **5**, 85–97.

79 J. Yan and S. Gao, Plasmon resonances in linear atomic chains: Free-electron behavior and anisotropic screening of d electrons, *Phys. Rev. B: Condens. Matter Mater. Phys.*, 2008, **78**, 235413.

80 N.,V. Karimova and C. M. Aikens, Time-Dependent Density Functional Theory Investigation of the Electronic Structure and Chiroptical Properties of Curved and Helical Silver Nanowires, *J. Phys. Chem. A*, 2015, **119**, 8163–8173.

81 Integrated DNA Technologies Fluorophores Modifications. Available at: http://www.idtdna.com/site/Catalog/Modifications/Dyes (accessed: 23rd August 2018).